Cancer Biology & Therapy 14:7, 606–613; July 2013; © 2013 Landes Bioscience

Bimodal role of Kupffer cells during colorectal cancer liver metastasis

Shu Wen Wen,[1,2,*] Eleanor I Ager,[1,3] and Christopher Christophi[1]

[1]Department of Surgery; The University of Melbourne; Austin Health; Heidelberg, Australia; [2]Tumor Microenvironment Laboratory; Queensland Institute of Medical Research; Herston, Australia; [3]Edwin L. Steele Laboratory for Tumor Biology; Massachusetts General Hospital and Harvard Medical School; Boston, MA USA

Keywords: macrophage, tumor-associated macrophages, Kupffer cell, liver metastases, colorectal cancer

Abbreviations: KC, Kupffer cell; CRC, colorectal cancer; $GdCl_3$, gadolinium chloride; VEGF, vascular endothelial growth factor; iNOS, inducible nitric oxide synthase; TAMs, tumor-associated macrophages (TAMs); SEM, standard error of the mean

Kupffer cells (KCs) are resident liver macrophages that play a crucial role in liver homeostasis and in the pathogenesis of liver disease. Evidence suggests KCs have both stimulatory and inhibitory functions during tumor development but the extent of these functions remains to be defined. Using KC depletion studies in an orthotopic murine model of colorectal cancer (CRC) liver metastases we demonstrated the bimodal role of KCs in determining tumor growth. KC depletion with gadolinium chloride before tumor induction was associated with an increased tumor burden during the exponential growth phase. In contrast, KC depletion at the late stage of tumor growth (day 18) decreased liver tumor load compared with non-depleted animals. This suggests KCs exhibit an early inhibitory and a later stimulatory effect. These two opposing functions were associated with changes in iNOS and VEGF expression as well as T-cell infiltration. KC depletion at day 18 increased numbers of $CD3^+$ T cells and iNOS-expressing infiltrating cells in the tumor, but decreased the number of VEGF-expressing infiltrating cells. These alterations may be responsible for the observed reduction in tumor burden following depletion of protumor KCs at the late stage of metastatic growth. Taken together, our results indicate that the bimodal role of KC activity in liver tumors may provide the key to timing immunomodulatory intervention for the treatment of CRC liver metastases.

Introductions

Resident liver macrophages (Kupffer cells; KCs) play a crucial role in the pathogenesis of liver disease and are a major component of the microenvironment of primary and metastatic liver tumors. Direct and indirect activation of KCs results in the production of growth factors and chemotactic cytokines capable of facilitating both anti- and pro-tumor effects.[1-3] Upon activation, KCs can prevent the outgrowth of liver metastases during early metastatic stages.[4-6] Administration of gadolinium chloride ($GdCl_3$) or Cl_2MDP-liposomes prior to tumor cell challenge—which depletes KC populations and inhibits their phagocytic function—induces an increase in the load of liver metastases in animal models of CRC liver metastases.[4-6] In contrast, activation of KCs with Zymosan decreases the number of liver metastases.[5] However, excessive macrophage infiltration has been correlated with poor prognosis in colon, breast, lung and prostate cancer.[7-12] KCs are capable of facilitating tumor growth through several mechanisms, including the release of pro-angiogenic and pro-inflammatory factors (e.g., VEGF, IL-8, IL-6, and TNF-α) and extracellular matrix modification.[13]

Although systemic and infiltrating macrophage populations have been extensively investigated,[14-17] few studies to date have demonstrated the bimodal role of KCs. In the present study, we evaluated the ability of KCs to either support or inhibit tumor growth during the progression of CRC liver metastases. In addition, we examined key processes and factors associated with tumor growth, including cancer cell apoptosis and numbers of $CD3^+$ T cells, as well as VEGF- and iNOS-expressing cells.

Results

Early KC depletion increased tumor growth. Mice were administered $GdCl_3$ before tumor induction (day 0) and culled at days 7, 16, and 21. Control animals received saline. Liver metastases were not visible macroscopically until day 16 in both $GdCl_3$ treated and control animals (**Fig. 1B**). KC depletion before tumor induction increased liver tumor burden at day 16 compared with controls as assessed by quantitative stereological analysis ($P = 0.001$; **Fig. 1A**). However, by day 21 this effect was no longer observed (**Fig. 1A**). The effectiveness of $GdCl_3$ was assessed by evaluating the extent of KC depletion and repopulation in the tumor-induced liver. KCs were able to repopulate from 3 days after depletion and repopulation was shown to be complete by day 16 (**Fig. S1**).

Late KC depletion decreased tumor growth. Next we evaluated the heterogeneity of KCs during progression of CRC liver

*Correspondence to: Shu Wen Wen; Email: ShuWen.Wen@qimr.edu.au
Submitted: 01/04/13; Revised: 04/04/13; Accepted: 04/07/13
http://dx.doi.org/10.4161/cbt.24593

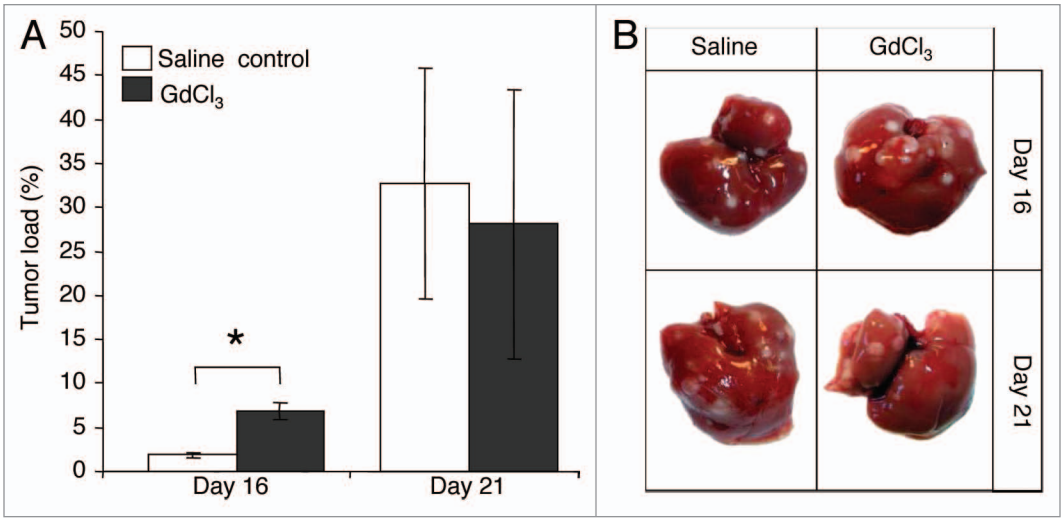

Figure 1. Early KC depletion (day 0) increases CRC liver metastases. (**A**) Animals were administered $GdCl_3$ at day 0 before induction of CRC liver metastases. Livers were collected at days 7, 16, and 21 after tumor induction. Liver metastases were not macroscopically visible until day 16. Tumor burden was assessed by quantitative stereological analysis as the percentage of tumor volume over total tumor-bearing liver volume. (**B**) Representative macroscopic images of tumor-bearing livers treated with either $GdCl_3$ or saline (control). Results are expressed as mean values ± SEM, $n = 6$ animals per group, $^*P = 0.001$.

metastases. Mice induced with CRC liver metastases were treated with $GdCl_3$ on one of days 0, 10, 14, or 18 and finally culled at day 21. Control animals received saline. KC depletion at the late stages of tumor growth (day 18) significantly decreased liver tumor load ($P < 0.001$; **Fig. 2A**) and the number of tumor nodules ($P = 0.001$; **Fig. 2B**) by day 21 compared with control. However, when KCs were depleted at the earlier growth stages (days 0, 10, and 14), both tumor load and the number of tumor nodules were not significantly changed (**Fig. 2A and B**). These results indicate that the effects of KC depletion on tumor burden are temporary and short-lasting.

Early KC depletion altered iNOS and VEGF expression in tumors but not CD3⁺ or apoptotic cells. The number of $CD3^+$ cells in the tumor remained at control levels when KCs were depleted at early time points (day 0, 10, and 14) (**Fig. 3A**). $CD3^+$ T cells accumulated around the tumor periphery and infiltrated into the tumor stroma (**Fig. 3B**). The number of iNOS-expressing cells was also unchanged by KC depletion at day 0, 10, or 14 in tumors (**Fig. 4A**).

Early KC depletion at day 0 and day 10 did not alter the number of VEGF-expressing cells in the liver compared with untreated controls at day 21 (**Fig. 5A**). However, tumor VEGF-expression at day 21 significantly decreased when KCs were depleted at day 10 ($P = 0.041$; **Fig. 5B**) and 14 ($P = 0.042$; **Fig. 5B**), with a similar trend observed for day 0 ($P = 0.082$; **Fig. 5B**) KC depletion compared with control.

Large areas of apoptosis in the tumor center were observed using an active caspase-3 marker (**Fig. 6D**). Analysis of active caspase-3 immunostaining revealed the number of apoptotic cells in liver (**Fig. 6A**) and tumor (**Fig. 6C**) were unaltered by KC depletion at day 0 and day 10 compared with control. However, KC depletion at day 14 resulted in an increase in the number of apoptotic cells in the liver compared with controls ($P = 0.030$; **Fig. 6A**).

Late KC depletion (exponential growth phase) decreased VEGF expression, but increased iNOS expression, CD3⁺ infiltrating cells and apoptosis. KC depletion at day 18 was associated with decreased VEGF expression in both the liver ($P = 0.036$; **Fig. 5A**) and tumors ($P = 0.005$; **Fig. 5B**) relative to untreated controls. In contrast, the number of iNOS-expressing and $CD3^+$ cells significantly increased in tumors following late stage KC depletion (day 18) compared with controls ($P = 0.030$; **Fig. 4A** and $P = 0.013$; **Fig. 3A**, respectively). Additionally, the number of apoptotic cells in the liver also increased when KCs were depleted at day 18 compared with controls ($P = 0.024$; **Fig. 6A and B**). In the tumor however, the number of apoptotic cells remained at control levels (**Fig. 6C and D**).

KC depletion did not alter tumor vessel density. Angiogenic blood vessels were stained using the marker CD34. Tumor blood vessels stained strongly compared with host vessels surrounding the tumor (**Fig. 7A**). KC depletion during the progression of CRC liver metastases did not alter the density of vessels in the tumor compared with non-depleted control tumors (**Fig. 7B**).

Discussion

Macrophages are highly heterogeneous cells. They are capable of releasing a complex repertoire of growth factors and cytokines in response to changing tumor microenvironments. In the present study, hepatic macrophages (KCs) were found to be an important component of the liver tumor microenvironment with a significant role in determining the growth of metastatic CRC cells. Importantly, KC function appears to be bimodal, with an early inhibitory and a later stimulatory effect during the progression of metastatic growth.

Tumor growth in this model of CRC liver metastases occurs in three key phases: early lag phase, late exponential growth

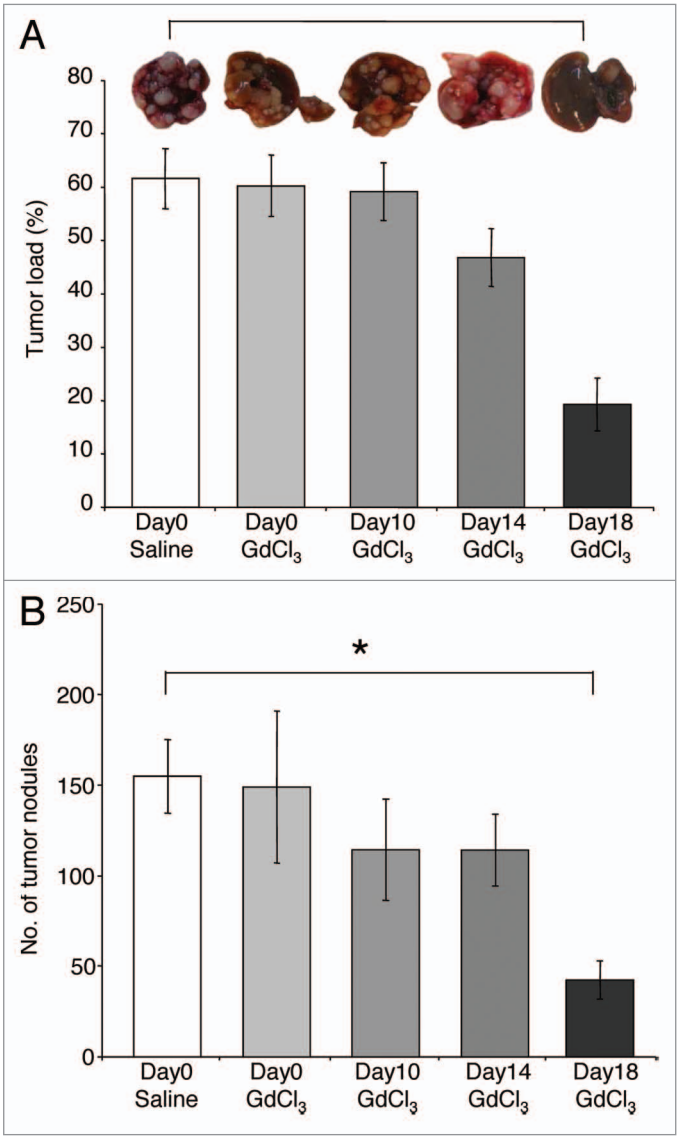

Figure 2. KCs display antitumor functions during established growth of CRC liver metastases. $GdCl_3$ was administered before tumor induction (day 0) or on one of days 10, 14, or 18 following tumor induction. Solubilizing agent (saline) provided a control. Livers were collected at day 21. Quantitative stereological methods were used to determine (**A**) the percentage of tumor volume over total tumor-bearing liver volume and (**B**) the number of tumor nodules per liver. Results are expressed as mean values ± SEM, $n = 6$ animals for each group, $^*P \leq 0.001$.

phase, and plateau phase.[18] In the present study, depletion of KCs early during tumor progression increases tumor burden, suggesting that these KCs are providing an antitumor effect. The findings are in agreement with Bayon et al. who demonstrated KC depletion strongly enhances tumor growth before day 14, but not at the later stages in an orthotopic rat model inoculated with syngeneic colon carcinoma cells.[19] In a syngeneic rat model, KCs were also shown to initiate high tumoricidal activity in conjunction with natural killer (NK) cells as early as 24 h after induction with CRC liver metastasis.[20]

KC's inhibition of tumor progression however, appears to be limited to the initial seeding and/or early growth periods. We showed that KC depletion during the later stages of tumor progression reduced tumor growth, suggesting that, at this stage, KCs have a protumor effect. Tumor-associated macrophages (TAMs) are known to participate in tumor immunosurveillance, angiogenesis, and to contribute to tumor progression and metastasis.[21-23] Indeed, the presence of TAMs in human studies has been linked with poor prognosis in patients with breast, prostate, bladder, and colon cancer.[12,24-26]

Contrary to the present findings, macrophages have also been shown to enhance both seeding and established metastatic growth. Using an orthotopic model of breast cancer metastasis to the lung, Qian et al. showed $CD11b^+$ macrophages were required for efficient tumor metastatic seeding and growth of metastatic nodules.[16] Recent studies have indicated that primary cancer cells may secrete factors that recruit macrophages to the secondary sites to create a pre-metastatic niche in which circulating tumor cells are stimulated to seed and expand.[27] Additionally, macrophages display considerable tissue heterogeneity, and this may explain their differential effects during tumor progression. While KCs are highly phagocytic, alveolar macrophages produce significantly greater quantities of reactive oxygen species and reactive-nitrogen intermediates, which can enhance tissue damage.[28]

KCs are a major source of VEGF expression in the liver tumor microenvironment and play an important role in regulating cancer progression through stimulating tumor angiogenesis and tumor cell invasion. However, it is unlikely that the antitumor effects of late KC depletion described here are solely due to the reduction in VEGF described. As evidence, we found that tumor VEGF-expression decreased when KCs were depleted at day 10, 14, and 18 with a similar trend observed for day 0. Therefore, VEGF reduction alone cannot explain the differences in tumor growth retardation achieved by KC depletion at the different stages. Genetic depletion of macrophages was shown to lower tumor vessel density and the progression to malignancy in polyoma middle T oncoprotein (PyMT)-induced mammary tumors.[29] This effect was reversed when the expression of VEGF was restored.[29] In the present study, a decrease in the number of VEGF-infiltrating cells did not correlate to changes in tumor vessel density, despite a decrease in overall tumor burden when depletion was performed close to the endpoint. This suggests other angiogenic effectors are able to compensate for the reduction in VEGF. However, parameters of vascular function, such as vessel permeability and perfusion, were not assessed here and may still be altered by the reduction in VEGF-infiltrating cells.

While VEGF-expressing cells were decreased by KC depletion at day 18, iNOS-positive infiltrating cells in tumors were increased. High iNOS concentrations can mediate cancer cell apoptosis and inhibit cancer growth.[30-33] The observed reduction in tumor burden and increase in apoptosis following late stage KC depletion in the present study may be due to a higher number of cells expressing iNOS in the tumor.

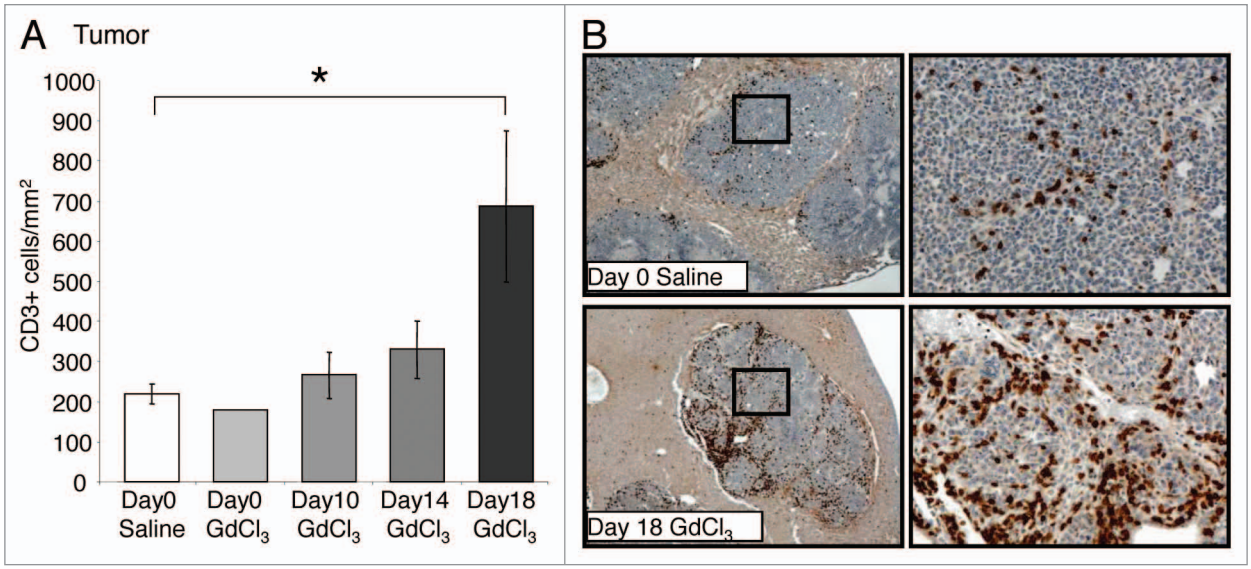

Figure 3. Depletion of KCs in established growth of CRC liver metastases increases T-cell numbers. Tumor-bearing mice were treated with $GdCl_3$ as described in **Figure 2**. Livers were collected at day 21. (**A**) $CD3^+$ T cells were identified using immunohistochemical staining and quantified as the number of positively stained cells/mm^2 in the tumor. Depending on the animal and its tumor load, 30–40 total images across 5–10 tumors were taken for analysis. (**B**) Representative images of $CD3^+$ staining in tumors of day 18 $GdCl_3$ treated animals compared with saline controls. T cells were stained brown and observed predominantly at the tumor host interface and in vascular lakes of the tumor. Results are expressed as mean values ± SEM, $n = 6$ animals per group, $^*P = 0.013$.

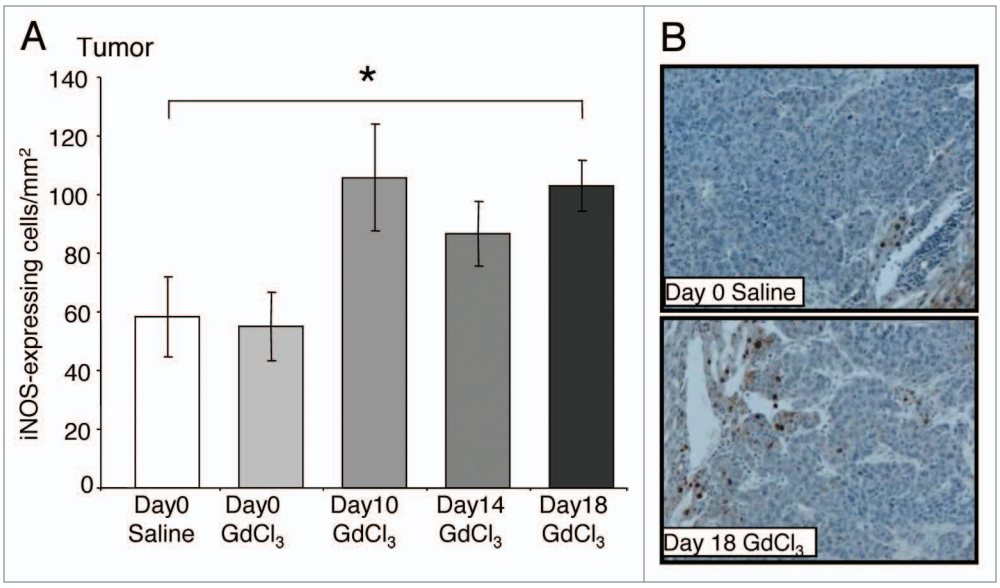

Figure 4. Depletion of KCs in established growth of CRC liver metastases increases iNOS-expressing cells. Tumor-bearing mice were treated with $GdCl_3$ as described in **Figure 2**. Livers were collected at day 21. (**A**) iNOS-expressing cells were identified using immunohistochemical staining and quantified as the number of positively stained cells/mm^2 in the tumor. Analysis are as described in the materials and methods. (**B**) Representative images of iNOS-expressing cells in tumors of day 18 $GdCl_3$ treated animals compared with saline controls. iNOS-expressing cells were stained brown and a majority of them were localized to the tumor host interface. Results are expressed as mean values ± SEM, $n = 6$ animals per group, $^*P = 0.03$.

A dramatically higher number of T cells in tumors following late KC depletion was observed. Increased T-cell infiltration in tumors is associated with a favorable prognosis in many cancer types.[34,35] TAMs can inhibit tumor-specific T-cell immunity by increasing T-regulatory cell numbers.[36] Therefore, depletion of TAMs in an established tumor microenvironment may help enhance T-cell mediated immunity to mediate an antitumor effect. However, further studies to define the subsets of T cells present in CRC liver metastases will be important before firm conclusions can be drawn on the interplay between TAM and the regulatory role of T cells on Th1 and Th2 responses during tumor progression.

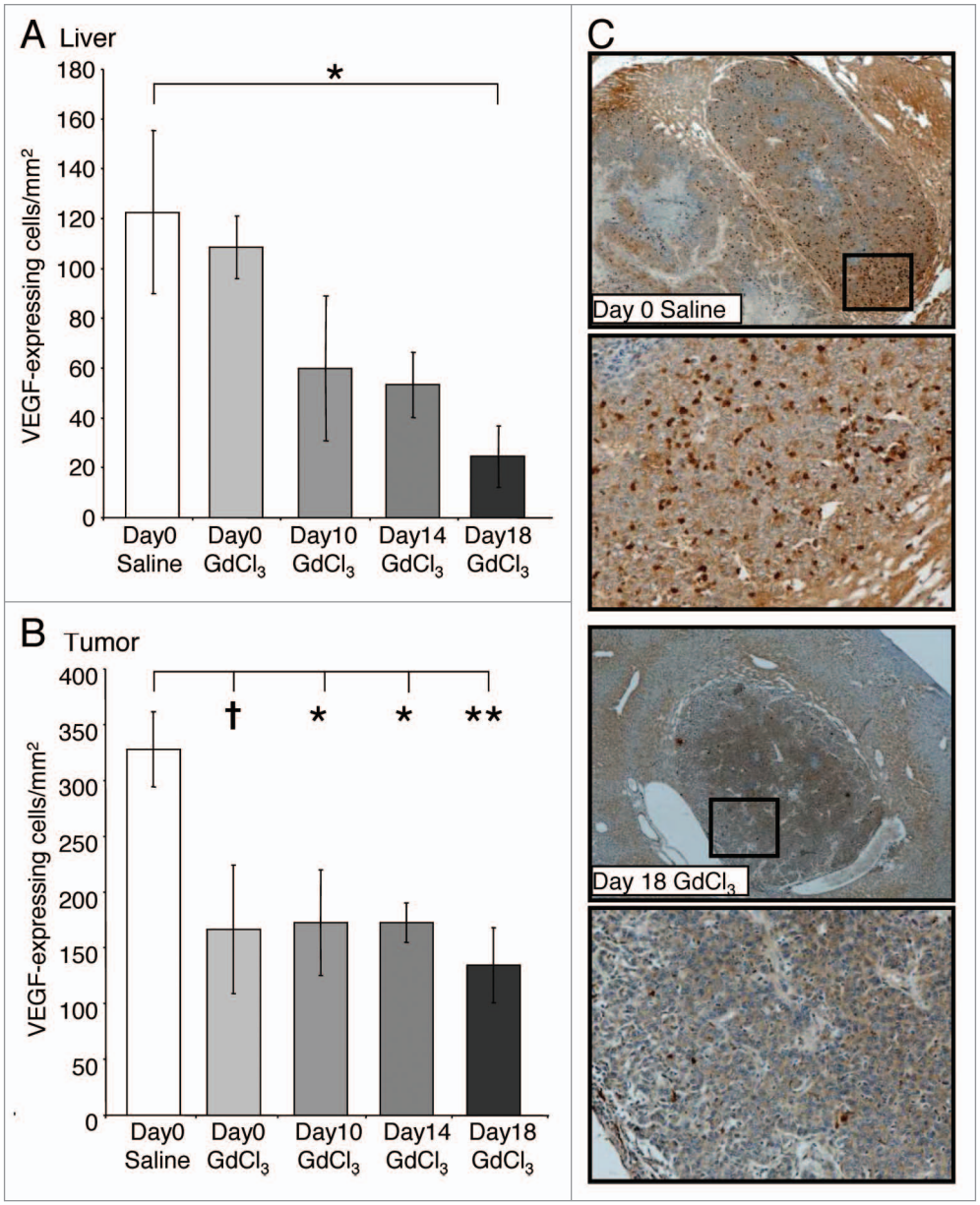

Figure 5. KC depletion decreases VEGF-infiltrating cells in both the liver and tumor in CRC liver metastases. Tumor-bearing mice were treated with $GdCl_3$ as described in **Figure 2**. Livers were collected at day 21. VEFG-expressing cells were identified using immunohistochemical staining and quantified as the number of positively stained cells/mm² in the (**A**) liver and (**B**) tumor. (**C**) Representative images of VEGF-expressing cells in tumors of day 18 $GdCl_3$ treated animals compared with saline controls. VEGF-expressing cells were stained brown. Results are expressed as mean values ± SEM, $n = 6$ animals per group. *$P < 0.05$, **$P < 0.01$, †$0.05 < P \leq 0.10$ considered a significant trend compared with saline control.

Materials and Methods

In vivo model and cell lines. The mouse colorectal cancer (MoCR) cell line used for in vivo experiments was harvested from a dimethylhydrazine-induced colon carcinoma in a CBA mouse at a stage known to metastasize to the liver.[18] CRC liver metastases were induced as described previously.[18,37] Briefly, a suspension of 2.5×10^4 MoCR cells were injected into the spleen of 6- to 8-week-old male CBA mice and, after three minutes, the spleen removed to confine metastases to the liver. In this model, angiogenesis is established by day 10, with a slow growth phase from days 10–16, a rapid growth phase until day 19, followed by a plateau phase.[18] A minimum of 6 animals per group were used. All experiments were approved by the Austin Health Animal Ethics Committee. Liver samples were collected and fixed in fresh 4% PFA.

Drugs/agents and treatments. KCs were depleted by two successive doses (6 to 24 h apart) of gadolinium chloride ($GdCl_3$; Sigma-Aldrich; 20 mg/kg) via tail-vein injection. $GdCl_3$ at this dose was previously determined to result in significant depletion of KCs.[38-41] $GdCl_3$ was administered before tumor induction (day 0) or on one of days 10, 14, or 18. The solubilizing agent

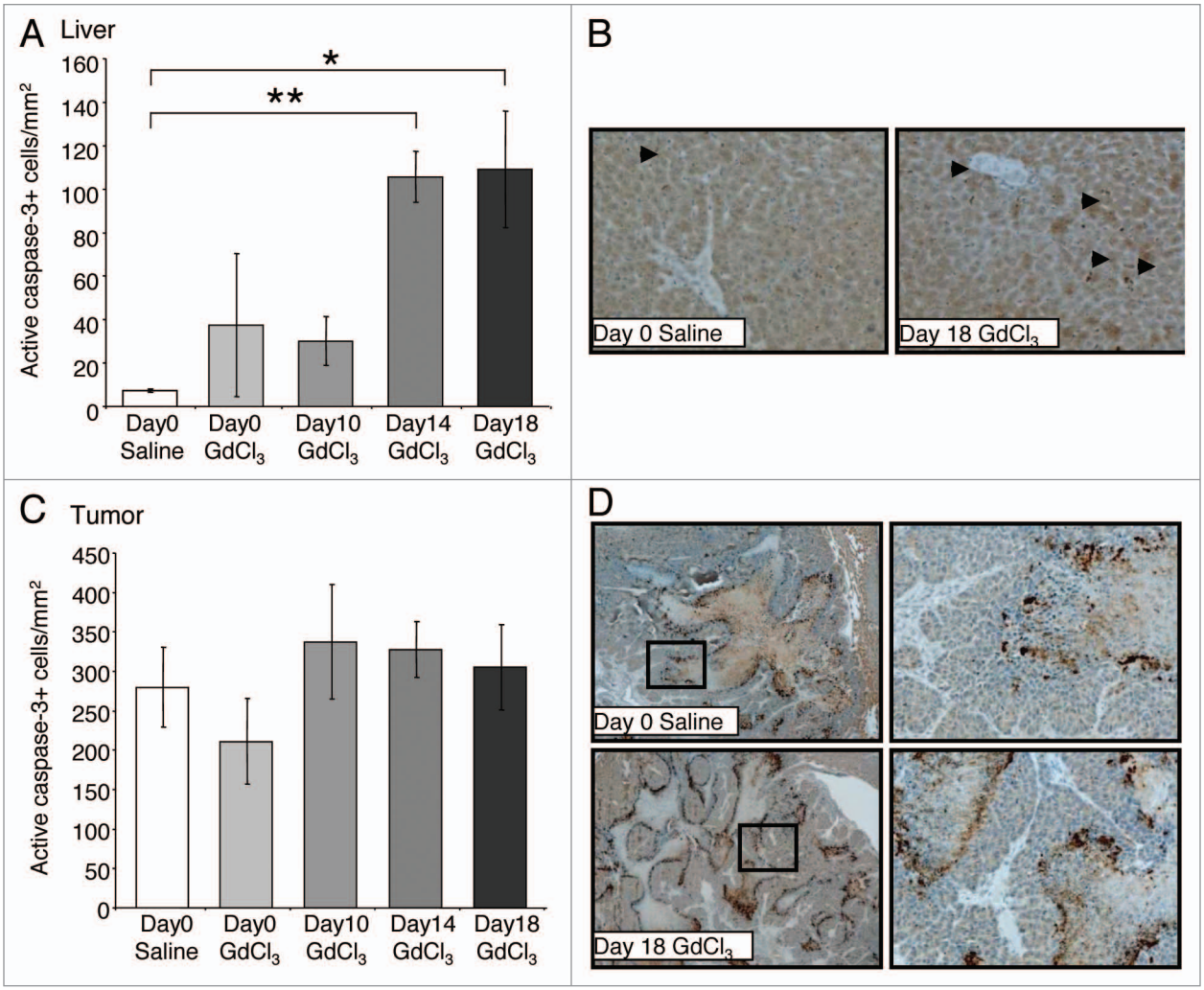

Figure 6. Effect of macrophage depletion on cell apoptosis in the liver and tumor. Tumor-bearing mice were treated with $GdCl_3$ as described in **Figure 2**. Livers were collected at day 21. (**A**) Apoptotic cells were identified using the active caspase-3 marker and quantified as the number of positively stained cells/mm² in the (**A**) liver and (**B**) tumor. (**C**) Representative images of active caspase-3 staining (brown-stained cells) showing apoptotic cells in the liver as indicated by arrows. (**D**) Apoptotic cells in the tumor general localized to the necrotic regions. Results are expressed as mean values ± SEM, $n = 6$ animals per group. *$P < 0.024$, **$P < 0.030$.

(saline) provided a control. Animals treated before induction of CRC liver metastases were sacrificed at days 7, 16, and 21. Animals treated on either day 10, 14, or 18 were sacrificed on day 21.

Tumor burden. Quantitative stereological analysis was performed on whole fixed livers collected at endpoints (day 7, 16, and 21) to determine tumor burden. The fixed livers were transversely sliced into 1.5 mm sections with a multi blade fractionator and an image of liver sections taken using Lumenera Infinity4 digital CCD camera. Tumor area (mm²) and the number of tumors per liver were assessed using Image-Pro plus 6.0. The areas were converted to volume measurements based on the thickness of each tissue slice (1.5 mm) and the proportion of liver sampled. This was subsequently used to calculate the percentage of tumor burden in the liver.

Immunohistochemical staining and analyses. Apoptosis (active caspase-3; rabbit polyclonal, R&D Systems *AF835*), angiogenesis (CD34 neovascularization marker; rat anti-mouse, Abd Serotec MCA18256), macrophages (F4/80; monoclonal rat anti-mouse, ATCC no HB-198, culture supernatant), T cells (CD3; rabbit anti-human, DAKO A0452), iNOS (rabbit anti-mouse Abcam ab3523), and VEGF (rabbit anti-mouse Abcam ab46154) were assessed in PFA-fixed paraffin embedded tissues. Active caspase-3 was used at the concentration of 1.0 μg/ml, CD34 at 0.1 μg/ml, F4/80 at a 1:20 000 dilution, CD3 at 0.6 μg/ml, iNOS at 13.3 μg/ml, and VEGF at 0.5 μg/ml. Non-immunized rabbit IgG (Santa Cruz, sc-2027), at an equivalent concentration to the primary antibody, was used as a negative control. For F4/80, VEGF, and iNOS, proteinase K (1 mg/ml) antigen retrieval at 37 °C was required. Endogenous peroxidases were blocked with 3% H_2O_2 and non-specific binding inhibited with 10% normal goat serum (Zymed, 01-6201). Slides were incubated with primary antibodies at 37 °C for 1 h and then 4 °C overnight. Slides were then incubated with the

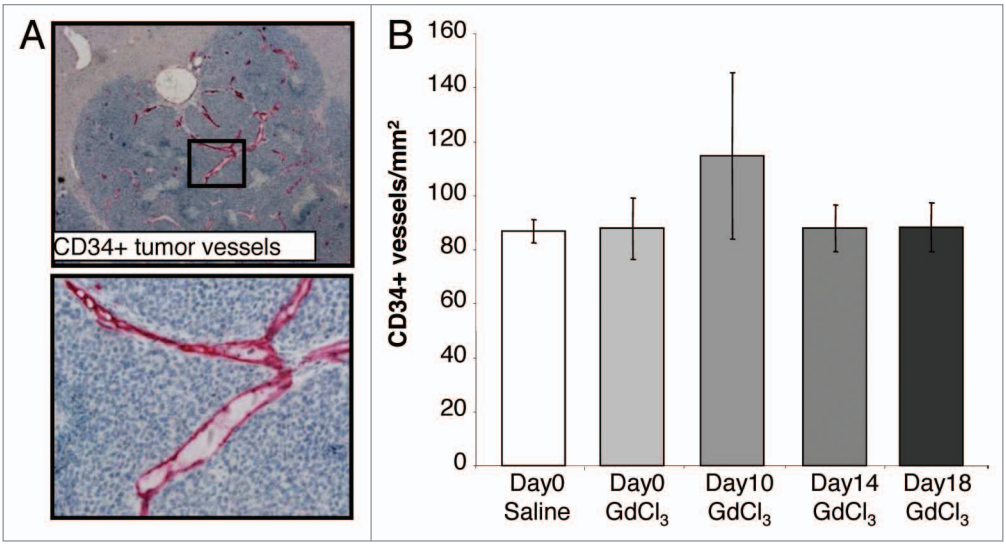

Figure 7. KC depletion does not alter the density of immature vessels. Tumor-bearing mice were treated with $GdCl_3$ as described in **Figure 2**. Livers were collected at day 21. (**A**) Representative images of $CD34^+$ staining on endothelial cells of immature blood vessels. $CD34^+$ cells were stained red. (**B**) Newly formed (angiogenesis) blood vessels were identified using the CD34 marker and quantified as the number of positively stained vessels/mm^2 in the tumor. Results are expressed as mean values ± SEM, $n = 6$ animals per group.

secondary antibody (Dako Envision+ goat anti-rabbit HRP secondary 4011) for active capase-3, F4/80, CD3, VEGF and iNOS and the Rat on Mouse AP-polymer kit (Biocare Medical; RT518H) for CD34. F4/80 required incubation with a linking polyclonal rabbit anti-rat biotinylated antibody (Dako Envision Plus) at 37 °C prior to the secondary antibody. Visualization was induced with diaminobenzidine (DAB) or, for CD34, Vulcan fast red (Applied Medical FR805H). Slides were counterstained with Mayer's hematoxylin.

For quantitation, stereological principles were followed. Representative images from immunohistochemically stained sections were captured using a digital light microscope (Nikon Coolscope, Nikon Corporation) at a magnification between 40× and 400×. Images were captured using a pattern which ensured unbiased selection and no overlap. Depending on the animal and its tumor load, 30–40 total images across 5–10 tumors were taken for analysis. Active caspase-3, F4/80, CD3, VEGF, and iNOS were assessed as the number of positively stained cells per high power area of tumor or liver (ImagePro-Plus Version 6.0). Tumor vessel density, which provides an indication of angiogenic potential, was determined by counting the number of CD34 positive vessels per tumor area.

Statistical analysis. Quantitative data are presented as means ± SEM. Statistical analyses were conducted using SPSS (Statistical Package for the Social Sciences, version 17). Data sets were tested for normality using the Kolmogorov–Smirnov test. Parametric data was analyzed using ANOVA with post-hoc comparison (Tukey method). Non-parametric data was analyzed using the Mann–Whitney U-test. Adjusted $P \leq 0.05$ was considered statistically significant and $0.05 < P \leq 0.10$ considered a significant trend.

Conclusion

The results presented here demonstrate the bimodal function of KCs during CRC liver metastasis. Understanding this switch in KC phenotype may allow for the development of therapies that extend the initial antitumor function of KCs into later stages of tumor growth.

Disclosure of Potential Conflicts of Interest

No potential conflict of interest was disclosed.

Acknowledgments

This work was supported by Cancer Australia's Priority-driven Collaborative Cancer Research Scheme (co-funded by Cancer Australia and Cure Cancer Australia Foundation) and by the Cancer Council of Victoria. Dr Ager was supported by an NHMRC Post-doctoral Training Award. SWW was supported by an Australian Rotary Health Research Fund PhD Scholarship.

Supplemental Materials

Supplemental materials may be found here:
www.landesbioscience.com/journals/cbt/articles/24593

References

1. Bilzer M, Roggel F, Gerbes AL. Role of Kupffer cells in host defense and liver disease. Liver Int 2006; 26:1175-86; PMID:17105582; http://dx.doi.org/10.1111/j.1478-3231.2006.01342.x
2. Paschos KA, Majeed AW, Bird NC. Role of Kupffer cells in the outgrowth of colorectal cancer liver metastases. Hepatol Res 2010; 40:83-94; PMID:19788686; http://dx.doi.org/10.1111/j.1872-034X.2009.00578.x
3. van der Bij GJ, Oosterling SJ, Meijer S, Beelen RH, van Egmond M. Therapeutic potential of Kupffer cells in prevention of liver metastases outgrowth. Immunobiology 2005; 210:259-65; PMID:16164033; http://dx.doi.org/10.1016/j.imbio.2005.05.020
4. Heuff G, Oldenburg HS, Boutkan H, Visser JJ, Beelen RH, Van Rooijen N, et al. Enhanced tumor growth in the rat liver after selective elimination of Kupffer cells. Cancer Immunol Immunother 1993; 37:125-30; PMID:8319242; http://dx.doi.org/10.1007/BF01517045
5. Pearson HJ, Anderson J, Chamberlain J, Bell PR. The effect of Kupffer cell stimulation or depression on the development of liver metastases in the rat. Cancer Immunol Immunother 1986; 23:214-6; PMID:3024833; http://dx.doi.org/10.1007/BF00205652
6. Rushfeldt C, Sveinbjørnsson B, Seljelid R, Smedsrød B. Early events of hepatic metastasis formation in mice: role of Kupffer and NK-cells in natural and interferon-gamma-stimulated defense. J Surg Res 1999; 82:209-15; PMID:10090831; http://dx.doi.org/10.1006/jsre.1998.5532
7. Hamada I, Kato M, Yamasaki T, Iwabuchi K, Watanabe T, Yamada T, et al. Clinical effects of tumor-associated macrophages and dendritic cells on renal cell carcinoma. Anticancer Res 2002; 22(6C):4281-4; PMID:12553070.
8. Hanada T, Nakagawa M, Emoto A, Nomura T, Nasu N, Nomura Y. Prognostic value of tumor-associated macrophage count in human bladder cancer. Int J Urol 2000; 7:263-9; PMID:10910229; http://dx.doi.org/10.1046/j.1442-2042.2000.00190.x
9. Leek RD, Landers RJ, Harris AL, Lewis CE. Necrosis correlates with high vascular density and focal macrophage infiltration in invasive carcinoma of the breast. Br J Cancer 1999; 79:991-5; PMID:10070902; http://dx.doi.org/10.1038/sj.bjc.6690158
10. Lissbrant IF, Stattin P, Wikstrom P, Damber JE, Egevad L, Bergh A. Tumor associated macrophages in human prostate cancer: relation to clinicopathological variables and survival. Int J Oncol 2000; 17:445-51; PMID:10938382.
11. Ohno S, Ohno Y, Suzuki N, Kamei T, Koike K, Inagawa H, et al. Correlation of histological localization of tumor-associated macrophages with clinicopathological features in endometrial cancer. Anticancer Res 2004; 24(5C):3335-42; PMID:15515429.
12. Tsutsui S, Yasuda K, Suzuki K, Tahara K, Higashi H, Era S. Macrophage infiltration and its prognostic implications in breast cancer: the relationship with VEGF expression and microvessel density. Oncol Rep 2005; 14:425-31; PMID:16012726.
13. Knittel T, Mehde M, Kobold D, Saile B, Dinter C, Ramadori G. Expression patterns of matrix metalloproteinases and their inhibitors in parenchymal and non-parenchymal cells of rat liver: regulation by TNF-alpha and TGF-beta1. J Hepatol 1999; 30:48-60; PMID:9927150; http://dx.doi.org/10.1016/S0168-8278(99)80007-5
14. Gordon S, Martinez FO. Alternative activation of macrophages: mechanism and functions. Immunity 2010; 32:593-604; PMID:20510870; http://dx.doi.org/10.1016/j.immuni.2010.05.007
15. Gordon S, Taylor PR. Monocyte and macrophage heterogeneity. Nat Rev Immunol 2005; 5:953-64; PMID:16322748; http://dx.doi.org/10.1038/nri1733
16. Qian B, Deng Y, Im JH, Muschel RJ, Zou Y, Li J, et al. A distinct macrophage population mediates metastatic breast cancer cell extravasation, establishment and growth. PLoS One 2009; 4:e6562; PMID:19668347; http://dx.doi.org/10.1371/journal.pone.0006562
17. Solinas G, Germano G, Mantovani A, Allavena P. Tumor-associated macrophages (TAM) as major players of the cancer-related inflammation. J Leukoc Biol 2009; 86:1065-73; PMID:19741157; http://dx.doi.org/10.1189/jlb.0609385
18. Kuruppu D, Christophi C, Bertram JF, O'Brien PE. Characterization of an animal model of hepatic metastasis. J Gastroenterol Hepatol 1996; 11:26-32; PMID:8672738; http://dx.doi.org/10.1111/j.1440-1746.1996.tb00006.x
19. Bayón LG, Izquierdo MA, Sirovich I, van Rooijen N, Beelen RH, Meijer S. Role of Kupffer cells in arresting circulating tumor cells and controlling metastatic growth in the liver. Hepatology 1996; 23:1224-31; PMID:8621157; http://dx.doi.org/10.1002/hep.510230542
20. Timmers M, Vekemans K, Vermijlen D, Asosingh K, Kuppen P, Bouwens L, et al. Interactions between rat colon carcinoma cells and Kupffer cells during the onset of hepatic metastasis. Int J Cancer 2004; 112:793-802; PMID:15386374; http://dx.doi.org/10.1002/ijc.20481
21. Allavena P, Sica A, Solinas G, Porta C, Mantovani A. The inflammatory micro-environment in tumor progression: the role of tumor-associated macrophages. Crit Rev Oncol Hematol 2008; 66:1-9; PMID:17913510; http://dx.doi.org/10.1016/j.critrevonc.2007.07.004
22. Condeelis J, Pollard JW. Macrophages: obligate partners for tumor cell migration, invasion, and metastasis. Cell 2006; 124:263-6; PMID:16439202; http://dx.doi.org/10.1016/j.cell.2006.01.007
23. Pollard JW. Tumor-educated macrophages promote tumour progression and metastasis. Nat Rev Cancer 2004; 4:71-8; PMID:14708027; http://dx.doi.org/10.1038/nrc1256
24. Forssell J, Oberg A, Henriksson ML, Stenling R, Jung A, Palmqvist R. High macrophage infiltration along the tumor front correlates with improved survival in colon cancer. Clin Cancer Res 2007; 13:1472-9; PMID:17332291; http://dx.doi.org/10.1158/1078-0432.CCR-06-2073
25. Komohara Y, Ohnishi K, Kuratsu J, Takeya M. Possible involvement of the M2 anti-inflammatory macrophage phenotype in growth of human gliomas. J Pathol 2008; 216:15-24; PMID:18553315; http://dx.doi.org/10.1002/path.2370
26. Shimura S, Yang G, Ebara S, Wheeler TM, Frolov A, Thompson TC. Reduced infiltration of tumor-associated macrophages in human prostate cancer: association with cancer progression. Cancer Res 2000; 60:5857-61; PMID:11059783.
27. Hiratsuka S, Watanabe A, Aburatani H, Maru Y. Tumor-mediated upregulation of chemoattractants and recruitment of myeloid cells predetermines lung metastasis. Nat Cell Biol 2006; 8:1369-75; PMID:17128264; http://dx.doi.org/10.1038/ncb1507
28. Laskin DL, Weinberger B, Laskin JD. Functional heterogeneity in liver and lung macrophages. J Leukoc Biol 2001; 70:163-70; PMID:11493607.
29. Lin EY, Li JF, Bricard G, Wang W, Deng Y, Sellers R, et al. Vascular endothelial growth factor restores delayed tumor progression in tumors depleted of macrophages. Mol Oncol 2007; 1:288-302; PMID:18509509; http://dx.doi.org/10.1016/j.molonc.2007.10.003
30. Brüne B. The intimate relation between nitric oxide and superoxide in apoptosis and cell survival. Antioxid Redox Signal 2005; 7:497-507; PMID:15706097; http://dx.doi.org/10.1089/ars.2005.7.497
31. Tarr JM, Eggleton P, Winyard PG. Nitric oxide and the regulation of apoptosis in tumor cells. Curr Pharm Des 2006; 12:4445-68; PMID:17168753; http://dx.doi.org/10.2174/138161206779010477
32. Tendler DS, Bao C, Wang T, Huang EL, Ratovitski EA, Pardoll DA, et al. Intersection of interferon and hypoxia signal transduction pathways in nitric oxide-induced tumor apoptosis. Cancer Res 2001; 61:3682-8; PMID:11325839.
33. Weigert A, Brüne B. Nitric oxide, apoptosis and macrophage polarization during tumor progression. Nitric Oxide 2008; 19:95-102; PMID:18486631; http://dx.doi.org/10.1016/j.niox.2008.04.021
34. Diederichsen AC, Hjelmborg Jv, Christensen PB, Zeuthen J, Fenger C. Prognostic value of the CD4+/CD8+ ratio of tumor infiltrating lymphocytes in colorectal cancer and HLA-DR expression on tumour cells. Cancer Immunol Immunother 2003; 52:423-8; PMID:12695859; http://dx.doi.org/10.1007/s00262-003-0388-5
35. Naito Y, Saito K, Shiiba K, Ohuchi A, Saigenji K, Nagura H, et al. CD8+ T cells infiltrated within cancer cell nests as a prognostic factor in human colorectal cancer. Cancer Res 1998; 58:3491-4; PMID:9721846.
36. Kryczek I, Wei S, Zhu G, Myers L, Mottram P, Cheng P, et al. Relationship between B7-H4, regulatory T cells, and patient outcome in human ovarian carcinoma. Cancer Res 2007; 67:8900-5; PMID:17875732; http://dx.doi.org/10.1158/0008-5472.CAN-07-1866
37. Neo JH, Malcontenti-Wilson C, Muralidharan V, Christophi C. Effect of ACE inhibitors and angiotensin II receptor antagonists in a mouse model of colorectal cancer liver metastases. J Gastroenterol Hepatol 2007; 22:577-84; PMID:17376054; http://dx.doi.org/10.1111/j.1440-1746.2006.04797.x
38. Hardonk MJ, Dijkhuis FW, Hulstaert CE, Koudstaal J. Heterogeneity of rat liver and spleen macrophages in gadolinium chloride-induced elimination and repopulation. J Leukoc Biol 1992; 52:296-302; PMID:1522388.
39. Kono H, Fujii H, Asakawa M, Yamamoto M, Maki A, Matsuda M, et al. Functional heterogeneity of the kupffer cell population is involved in the mechanism of gadolinium chloride in rats administered endotoxin. J Surg Res 2002; 106:179-87; PMID:12127824; http://dx.doi.org/10.1006/jsre.2002.6434
40. Maher JM, Aleksunes LM, Dieter MZ, Tanaka Y, Peters JM, Manautou JE, et al. Nrf2- and PPAR alpha-mediated regulation of hepatic Mrp transporters after exposure to perfluorooctanoic acid and perfluorodecanoic acid. Toxicol Sci 2008; 106:319-28; PMID:18757529; http://dx.doi.org/10.1093/toxsci/kfn177
41. Mizgerd JP, Molina RM, Stearns RC, Brain JD, Warner AE. Gadolinium induces macrophage apoptosis. J Leukoc Biol 1996; 59:189-95; PMID:8603991.